ELSEVIER

Journal of Alloys and Compounds 253–254 (1997) 406–413

Journal of ALLOYS AND COMPOUNDS

Modelling of hydrogen behavior in metals by muons

A. Schenck

Institute for Particle Physics of ETH Zürich, CH-5232 Villigen PSI, Switzerland

Abstract

Positive muons substituting for protons in metals can be used to study various aspects of the behavior of hydrogen in metals and associated changes in the properties of the host material: this concerns e.g. the hydrogen (muon) lattice site, lattice relaxation, charge screening, diffusion as well as hydrogen induced changes in magnetic properties etc. Relevant examples are presented.

Keywords: μ^+ in metals

1. Introduction

Although positive muons (μ^+) belong to the family of leptons, like electrons and neutrini, when implanted in matter they have much more in common with the proton and its heavier isotopes, having the same charge and a mass of ~1/9 the proton mass (m_p), rendering the μ^+ the lightest isotope of the hydrogen family. In contrast the positron with a mass ~1/1800 m_p behaves quite differently in matter and has much more in common, as far as its dynamics is concerned, with its antiparticle, the electron. In many insulators, semiconductors and liquids implanted positive muons will capture an electron to form the analogue of atomic hydrogen, the atom muonium (μ^+e^-). The electron binding energy and the Bohr radius are practically the same as in atomic hydrogen, so also from a chemical point of view the positive muon can serve as a proton substitute. For the role of positive muons and/or muonium in semiconductors see the contribution of Cox and Lichti [1].

In metals, however, muonium, as well as atomic hydrogen, is unstable and does not form due to the presence of the many conduction electrons which jointly screen the μ^+'s or proton's positive charge. Nevertheless the actual electron charge distribution may resemble that of atomic hydrogen to quite some extent at least in simple s-electron metals [2].

One very important aspect of hydrogen behavior in metals concerns its diffusive motion. Being a relatively light particle hydrogen diffusion will be dominated by quantum effects which are known to depend sensitively on the particle mass. Here the availability of μ^+ has greatly extended the accessible mass range from 3 m_p for tritium down to 1/9 m_p for μ^+. Indeed the study of muon diffusion has contributed enormously to our present understanding of quantum diffusion of light interstitials and of the most important mechanisms involved (for reviews see Refs. [3–5]).

Another notable aspect is that μ^+ can be implanted in any kind of material, including metals and intermetallic compounds which usually do not take up hydrogen or have only extremely small hydrogen solubilities, thus extending the number of systems in which the behavior of at least isolated muons/protons can be studied to an essentially unlimited value.

The technique of experimentally observing the μ^+ behavior in metals is known as muon spin rotation–relaxation–resonance (μSR) spectroscopy. For details the interested reader is referred to e.g. Ref. [6]. μSR spectroscopy has much in common with NMR or $\gamma\gamma$PAC and one measures basically the same parameters, namely energy splittings, e.g., the Zeeman frequency (Knight shift), relaxation rates ($1/T_1$, $1/T_2$) and inhomogeneous line broadening. In contrast to NMR this can be done also in zero external field. Such data can then be used to determine the μ^+-site and local lattice relaxation, the pile up of electron charge at the μ^+, the short and long range diffusion (tunnelling) of the μ^+, correlation effects in metal hydrides and last but not least induced effects on the host lattice system.

2. μ^+-Site and local lattice relaxation

Pertinent information can be obtained from measurements of the inhomogeneous line broadening yielding the

0925-8388/97/$17.00
PII S0925-8388(96)02942-8

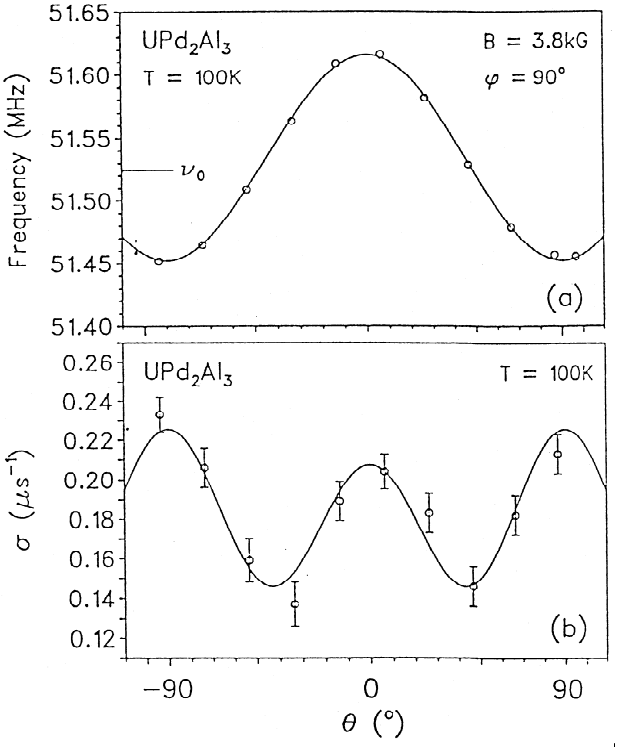

Fig. 1. Angular dependence of μ^+-Knight shift and depolarisation rate ($=\sqrt{M_2/2}$) in UPd_2Al_3. The solid lines reproduce the expected angular dependencies for the b-site [7,8].

second moment M_2 of the nuclear dipolar field distribution at the μ^+ (only possible if the host lattice nuclei carry a spin and magnetic dipole moment) and/or from the anisotropic contribution to the μ^+-Knight shift K_μ arising from the dipolar fields of external-field induced electronic moments at the host atoms (this requires usually single crystals and is best achieved in strongly paramagnetic compounds; it works only if the μ^+-site has a non-cubic local symmetry). Further, in magnetically ordered systems the observed spontaneous hyperfine field at the μ^+-site, in so far that it contains a dipolar contribution, may serve to determine the μ^+-site as well. Both the second moment as well as the anisotropic Knight shift depend very sensitively on the involved site and usually allow us to unambiguously determine this site. As an example Fig. 1 shows results on the angular dependence of both M_2 and the muon Knight shift in UPd_2Al_3, isostructural to $LaNi_5$ [7,8]. The solid lines represent calculations for the b-site which are in excellent agreement with the data. Other site assignments result in predictions totally incompatible with the data. Table 1 presents an incomplete list of determined μ^+-sites in compounds of quite different structures. In those compounds, in which the proton site is also known, the μ^+ is always found at the same site. It is interesting to note that the μ^+-site in the hexagonal $CaCu_5$ structure is not generally the same.

A precise comparison of measured and calculated angular dependencies of M_2 and/or K_μ provides also a measure of the local lattice relaxation around the μ^+. Generally a lattice expansion around the μ^+ is observed (see Table 1), a possible exception seems to be present in Bi, where a reduction of the μ^+–nearest Bi distance of ~10% is extracted from the data [24]. It appears that the lattice relaxation around the μ^+ may be slightly larger than around a proton (e.g. in Nb). This may be traced back to the larger zero point vibration amplitude of the lighter μ^+.

Second moment measurements can also be used to study the proton–muon spatial arrangement in metal hydrides. This is particularly feasible in systems where only the proton carries a sizable magnetic moment and contributes

Table 1
Compilation of μ^+-sites in various compounds (not complete)

System	Crystal structure	μ-Site	Source	Nearest neighbor displacement	Ref.
Cu	fcc	Octahedral[a]	M_2	<(2-5)%	[9,10]
Al	fcc	Tetrahedral/octahedral[b]	M_2		[11]
Nb	bcc	Tetrahedral[a]	M_2	≤6.7%	[12]
Fe	bcc	Tetrahedral	B_{hf}, $1/T_1$, $1/T_2$		[13]
Co	hcp	Octahedral	B_{hf}		[14]
Sc	hcp	Tetrahedral[a]	M_2	~0%	[15]
In	Tetragonal	Tetrahedral	M_2	<10%	[16]
$PdH_{\leq 1}$	fcc	Octahedral[a]	M_2		[17]
$TiH_{\sim 2}$	fcc, fct	Tetrahedral[a]	M_2	~3%	[18]
		+ octahedral		~7%	
CeAs	Cubic (NaCl)	Tetrahedral	K_μ		[19]
$CeAl_2$	Cubic (C_{15})	(2-2) site	M_2		[20]
$ErNi_5$	Hexagonal ($CaCu_5$)	f-site	K_μ		[21]
$PrNi_5$	Hexagonal ($CaCu_5$)	i-site[c]	K_μ		[22]
UPd_2Al_3	Hexagonal ($CaCu_5$)	b-site	K_μ, M_2	(1-6)%	[7]
CeB_6	Cubic (Pm $\bar{3}$m)	d-site (0 0 1/2	K_μ		[8]
$CeCu_6$	Orthorhombic	b-site (0 0 1/2)	K_μ	~9%	[8]
$CeRu_2Si_2$	Tetragonal	b-site (0 0 1/2)	K_μ	~3%	[8]
$HoNi_2B_2C$	Body centered tetragonal	(0 0 0.2)	K_μ		[23]

[a] same site is found for protons, [b] trap related sites, [c] nearly same site found for protons in $LaNi_5$.

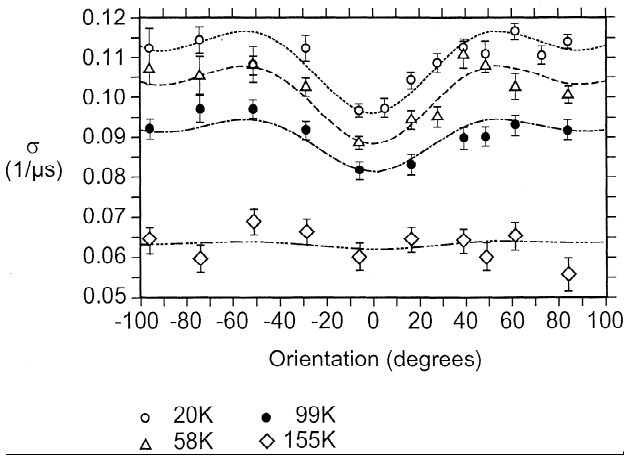

Fig. 2. Angular dependence of the μ^+ relaxation rate $\sigma=\sqrt{M_2/2}$ in $PdH_{0.74}$ for various temperatures. Note the almost complete disappearance of the anisotropy at 155 K while the average σ is only reduced by less than a factor of 2 [17].

dominantly to M_2. Fig. 2 shows the angular dependence of the relaxation rate $\sigma=(M_2/2)^{1/2}$ in a single crystal of $PdH_{0.74}$ for various temperatures [17]. The 20 K curve implies that both the μ^+ and the neighboring protons occupy octahedral sites in the fcc-structure of Pd. The nearest neighbor proton shell consists of twelve sites in total but only ~75% of them are actually occupied by protons in agreement with the composition $PdH_{0.74}$. As can be seen in Fig. 2 the isotropic part of σ decreases with increasing temperature (by a factor of 1.75 from 20 K to 155 K) but the anisotropic part is reduced much more strongly. The latter observation implies that the overall reduction of σ is only in part caused by μ^+ and proton diffusion (see Section 3) but reflects an increasing depopulation of the nearest neighbor proton shell. A possible explanation is that the μ^+–proton interaction is repulsive and that the μ^+ prefers to reside in a proton depleted area which it may find more quickly at elevated temperatures. Consistent with this explanation is another observation, namely that the measured M_2 (μ^+) in PdH_x seems to saturate for $x\geq 0.75$ [25], i.e., the nearest neighbor proton shell seems never to assume the full stoichiometric configuration. It may be expected that in PdH_x with smaller hydrogen concentrations the repulsive μ^+–proton interaction is less important and indeed in a $PdH_{0.657}$ single crystal no change in the local μ^+–proton arrangement was evident [26].

3. Charge screening of the μ^+

The pile up of electronic charge around the μ^+ (or the proton), shielding its positive charge over a distance of the order of a Bohr radius, can be studied by measuring the μ^+-Knight shift. The latter is proportional to the charge enhancement (or more precisely to the spin density enhancement). Systematic studies of the muon Knight shift some years ago in simple s-electron metals [27] were well reproduced by so called spherical solid model jellium calculations [28], proving the ''screened proton'' model as opposed e.g. to the hydride anion model.

An interesting result was obtained in Zn prepared to contain monovacancy clusters (small voids), at which defects the μ^+ were trapped [29]. In this case a relatively large negative Knight shift of −520 ppm was observed (as compared to +60 ppm in defect free Zn) pointing perhaps to the formation of an extremely shallow and weakly bound paramagnetic state. This observation still awaits its proper theoretical explanation.

Information on the spatial structure of the screening cloud around the μ^+/proton can be obtained from a measurement of the electric field gradients at the nearest neighbor nuclei, affecting the quadrupolar hyperfine interaction of these neighbor nuclei [30,9]. An elegant technique to measure such an effect is what is called avoided level crossing spectroscopy in μSR. It exploits the fact that polarisation can be transferred from the μ^+ to the surrounding nuclei in the case that the Zeeman splitting of the μ^+ is degenerate with one of the possible hyperfine splitting transitions [31]. Such measurements have been in particular performed on μ^+ implanted in Cu [10]. Electric field gradients have been studied in more detail in Sc and in ScH_x [15].

4. μ^+ Diffusion

Most studies of the μ^+ behavior in metals concern its diffusional behavior which can be deduced from the line narrowing of the μSR signal [6]. Interest was focused in particular on the undisturbed intrinsic diffusion and the elucidation of the quantum effects involved. Here the results in Cu and Al opened up indeed a new chapter in our understanding of the quantum nature of the diffusion of light interstitials. The key observation, first made by Camani et al. [32] and Hartmann et al. [33], is contained in Fig. 3 which displays the temperature dependence of the μ^+ hopping rate in Cu [10]. As can be seen after first decreasing with decreasing temperature the hopping rate increases again as the temperature is lowered below ~60 K and reaches a nearly temperature independent rate below ~0.2 K. As can be also seen, the temperature dependence assumes quite different forms for different temperature regions. Starting from high temperatures down to $\sim 10^2$ K the hopping rate ν follows a temperature activated Arrhenius behavior

$$\nu = \nu_0 \exp(-E_a/kT)$$

consistent with the well established picture of phonon assisted tunnelling of a small polaron (μ^+/p + local

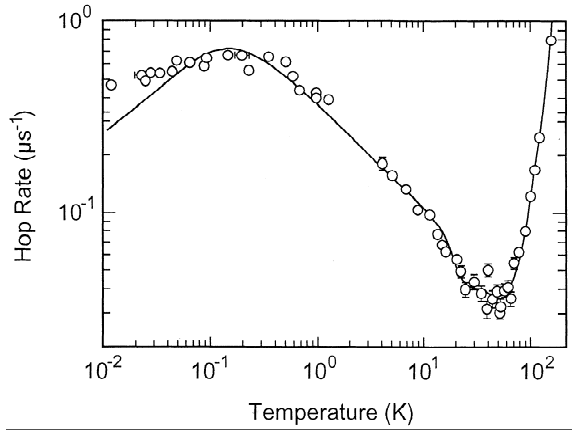

Fig. 3. Temperature dependence of μ^+ hopping rate in Cu [10].

lattice relaxation). In this model the preexponential factor is given by:

$$\nu_0 = J_0^2\left(\frac{\pi}{4\hbar^2 E_a kT}\right)^{1/2}$$

where J_0 is the bare tunnelling matrix element of the small polaron. For Cu one finds $J_0 \approx 36$ μeV and $E_a \approx 65$ meV. As the temperature is lowered further the multi phonon assisted tunnelling changes to a two phonon ($\nu \sim T^7$) and one phonon ($\nu \sim T$) assisted mode. Below ~60 K the rise of ν with decreasing T signals that yet another regime has set in which is thought to reflect the onset of a band like propagation of the particle. However, the life time of the band state is severely limited by non linear coupling phonon scattering, so called dynamical destruction, to the extent that the free mean path of propagation is always less than the lattice constant [34]. Hence the motion has still to be viewed as incoherent hopping. According to Ref. [34] for $T \ll \theta_D$ the hopping rate in this case should follow a power law behavior of $\nu \sim T^{-7}$ (or T^{-9}). Just below 30–40 K the data seem indeed to obey this prediction but then change to a much weaker temperature dependence from 10 K down to 500 mK, described by $\nu \sim T^{-\alpha}$ with α in the range $\alpha = 0.55$–0.67 [10,35]. This small exponent could not be explained on the basis of quantum theories taking only the particle–phonon interaction into account. A new mechanism had to be involved. This mechanism was identified to be electronic in origin [36,37]. When the μ^+ or proton tunnels from one interstitial site to the next one not only the lattice distortion (polaron) has to be shifted to the next site but also the electron screening cloud around the particle. This has two consequences. First, the tunnelling matrix element, now containing a factor describing the overlap of the wave functions representing the screening cloud before and after the jump, assumes a temperature dependence of T^{2K}, where K is a measure of the particle electron interaction (always $K \leq 0.5$). According to this law no diffusion should be possible in the zero temperature limit (orthogonality catastrophe). Secondly, the life time of the propagating muon state is again shortened due to interactions with the conduction electrons, leading to another factor proportional to T^{-1}. Altogether we find a T^{2K-1} dependences with $2K-1<0$. Experimentally $-\alpha = 2K-1 \sim -0.6$ and hence $K \approx 0.2$ [10,35].

Below ~0.5 K, where ν levels off and displays a tendency to decrease again yet another regime appears to take over. This is explained in terms of a spread of the muon's energy levels due to some intrinsic disorder [36] most probably arising from lattice defects (e.g. dislocations) and some residual impurities. E.g. when alloying Cu with 100 ppm Fe the hopping rate below 0.2 K is essentially suppressed to zero [37]. The strong influence of the conduction electrons on the μ^+ diffusion at very low temperatures as observed in Cu and also in Al [11] is in part due the ease with which electrons can be excited above the Fermi energy, allowing for low energy inelastic scattering. This should be drastically different in a superconductor where the energy gap prevents any low energy excitations of electrons. Indeed μ^+ diffusion in normal conducting and superconducting Al turned out to be quite different [38] (see Fig. 4). In normal conducting Al the μ^+ hopping rate shows an upturn below about 5 K essentially, very similar to the case in Cu and can be described also by the form T^{2K-1} with $2K-1 \approx -0.6$. In contrast in superconducting Al the hop rate rises very steeply. The difference in behavior can be traced back to the life time shortening term T^{-1} which in the superconducting state has to be replaced by $\Omega^{-1}(T) = [T/(1+\exp(\Delta_s(T)/k_B T))]^{-1}$ which reflects the reduced probability of finding free conduction electrons above the superconducting gap $\Delta_s(T)$. This result suggests that in those parts of the sample where the spread in μ^+ energy levels is small compared with $k_B\Omega(T)$ a truly coherent μ^+-state with band like features should develop at low T in the superconducting state.

The just described diffusion phenomena are not restricted to the light proton isotope, the μ^+, but have been

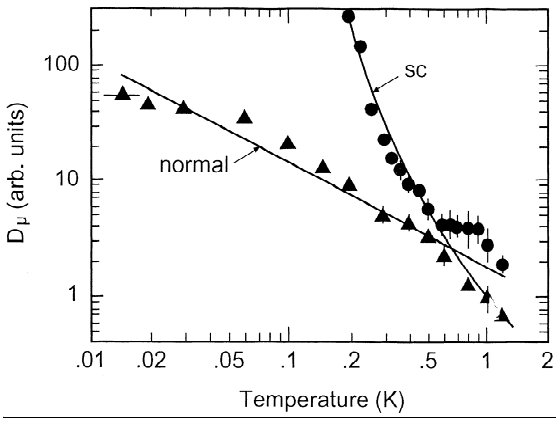

Fig. 4. Temperature dependence of μ^+ diffusion constant in normal and superconducting Al [5].

also observed for protons in the case of local motion between two sites separated by only a low potential barrier. The latter condition is necessary to obtain large enough tunnelling matrix elements in view of the protons much larger mass. Measurements in Sc and Y single crystals [39] revealed a proton hopping rate which developed a minimum at ~80 K and a $T^{-\alpha}$ (with $\alpha<1$)-dependence below 80 K. Even before the μSR measurements in superconducting Al, it was found that the two level tunnelling of protons in Nb in the vicinity of a nitrogen trap showed a weaker broadening of the tunnelling levels in the superconducting than in the normal state [40].

Forms of locally restricted tunnelling have occasionally been found also for μ^+ in metals, e.g., in the semimetal Bi between 20 K and 70 K the μ^+ performs some rapid temperature independent motion along the quasi open channels of the distorted simple cubic lattice of Bi [24]. It thereby seems that the extension of this local motion is determined by the level of impurities and is limited to just a few lattice spacings. Rapid tunnelling of the μ^+ between two adjacent tetrahedral sites in hcp Sc seems to have been observed as well [15].

5. Correlated μ^+–proton diffusion in metal hydrides

In metal hydrides with a nearly fully occupied hydrogen sublattice muon motion will be severely inhibited due to blocking by the protons [41]. The μ^+ will only be able to jump to the nearest equivalent site if the proton there has moved away first. This leads one to expect that the μ^+ diffusion rate should closely follow the proton's diffusion rate. However, studies in $LaNi_5H_6$ [25], $TiH_{\sim 2}$ [18], Zr_2NiH_x ($x=3$, 4.8) [42], $VH_{0.5}$ [43], CeH_x ($x=2.7$, 2.95) [44] and PdH_x ($x=0.70$, 0.75) [17] have produced the surprising result that the μ^+ diffusion rate is always smaller than the proton diffusion rate, at least above the temperature where proton diffusion sets in. As an example Fig. 5 displays the proton and muon hopping rates observed in $LaNi_5H_6$. Considering that the μ^+ hopping rates in TiH_2, Zr_2NiH_x, CeH_x and PdH_x are measured with respect to the hydrogen sublattice (only the protons possess magnetic moments of sufficient strength!) one may speculate that the proton–μ^+ motion is highly correlated, i.e., the μ^+ and some of the nearest proton neighbors move essentially together. On the other hand in $LaNi_5H_6$ and $VH_{0.5}$ the μ^+ motion is measured essentially with respect to the metal sublattice and the above argument cannot be applied. Taken at face value it seems that the μ^+ immobilizes its nearest neighbor protons. One may speculate that such an effect could result from the somewhat larger lattice relaxation induced by the μ^+ which in turn could act as a trapping potential for the protons. In summary, at present no convincing explanation exists and further measurements are eagerly awaited.

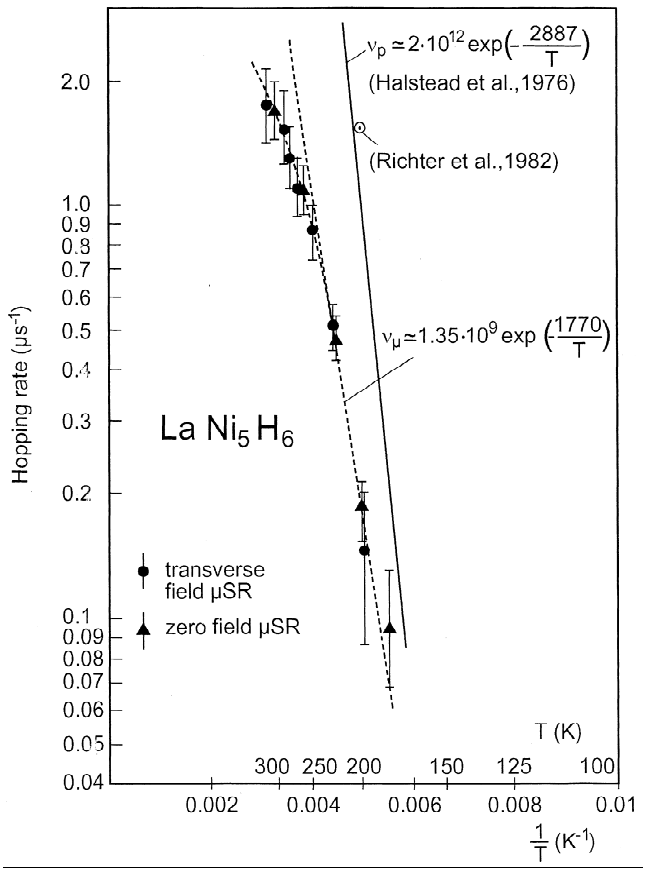

Fig. 5. Comparison of μ^+ and proton hopping rates in $LaNi_5H_6$ [25].

6. Muon (proton) induced changes of host lattice properties

The formation of metal hydrides has pronounced consequences on other properties of the host metal system and concern structural, electronic and magnetic features. With muons it is possible to study incipient features in the infinite dilute concentration limit. So far this has been exploited with respect to magnetic properties in intermetallic compounds. The first example shows how the presence of the muon (or proton) changes the exchange coupling between the two nearest neighbor Ce^{3+}-ions in CeB_6 (see Table 1). This can be deduced from a measurement of the μ^+-Knight shift K_μ and its temperature dependence. Fig. 6 displays a Curie plot of K_μ^{-1} versus temperature [8]. From the zero Knight shift intercept one deduces an effective Curie temperature of $\theta_c=-1.5$ K which has to be contrasted with $\theta=-6$ K following from the magnetic susceptibility χ. Since the μ^+-Knight shift is dominantly induced by the two nearest Ce^{3+}-neighbors, K_μ reflects the atomic susceptibility of these neighbors. The reduction of the ''local'' θ_c in the presence of the μ^+ implies a weakening of the AF-exchange between the two nearest neighbors. One reason for this could be that the distance between these two Ce^{3+}-ions has increased.

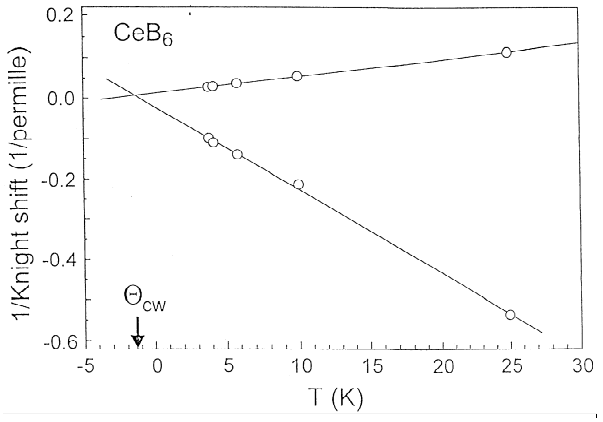

Fig. 6. Plot of reciprocal μ^+-Knight shift versus temperature in CeB_6. The external field was applied along a [1 0 0] axis. Since there are two magnetically inequivalent d-sites two different shifts are actually seen. The common zero intercept determines the effective paramagnetic Curie temperature [8].

Another reason may be that the pile up of conduction electron charge around the μ^+ has actually reduced the overlap between conduction electrons and the 4f-electron wave functions, thereby weakening the RKKY-coupling of the two Ce^{3+}-spins. Whatever the true explanation may be, the result suggests that the incorporation of hydrogen in CeB_6 should suppress the antiferromagnetic order in this system which develops below $T_N = 2.3$ K.

The second example concerns the effect of even a single μ^+ (or proton) on the crystalline electric field (CEF) splitting of nearest neighbor rare earth ions and the concomitant change in the atomic magnetic susceptibility. This effect appears to be most pronounced if the rare earth ion possesses a singlet ground state and the magnetic susceptibility is of the Van Vleck type. In this case there is a strong deviation of the local atomic susceptibility from the undisturbed one which becomes manifest when one compares the temperature dependence of the Knight shift (K_μ) and of the magnetic susceptibility. Since the Knight shift is a measure of the local susceptibility, as stated above, and if the local susceptibility is following the bulk susceptibility χ_b, one expects K_μ to scale with χ_b. Fig. 7 displays results obtained in the singlet ground state system $PrNi_5$ [22]. As can be seen K_μ scales with χ_b only above 60 K, while below all scaling is lost even to the extent that a change in sign of K_μ shows up. These results can be consistently understood if one allows for a change of the crystal field splitting of the $^3H_4$ multiplet of the two nearest Pr^{3+} neighbors (for the μ^+-site see Table 1). A perfect description of the data is achieved with the modified CEF splitting shown in Fig. 8. Only two CEF parameters B_2^0 and B_2^2 change from 0.51 meV and 0 meV to 0.555 meV and 0.085 meV, respectively, while all others (B_4^0, B_6^0, B_6^6) remain unchanged [22]. The effect of the presence of the μ^+ (or a proton) on the CEF splitting may be of two origins. First, the μ^+ induced lattice relaxation

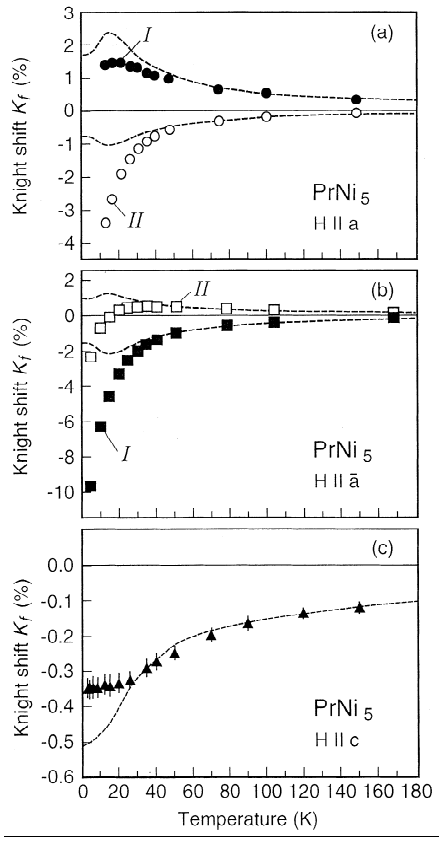

Fig. 7. Temperature dependence of μ^+-Knight shift and magnetic bulk susceptibility χ (dashed lines), normalized to K_μ at room temperature. Below 60 K the scaling of K_μ with χ is lost [22].

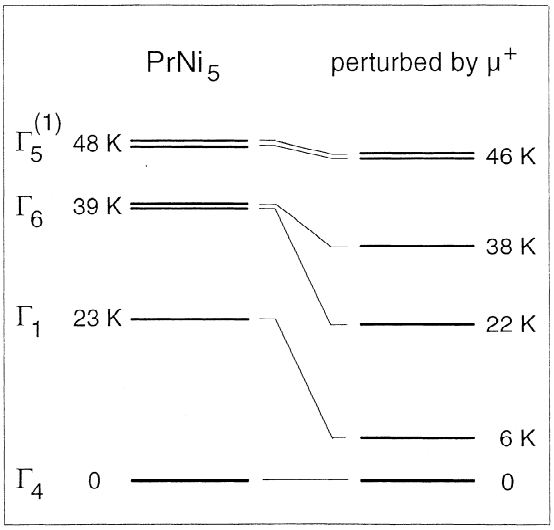

Fig. 8. CEF level scheme for $PrNi_5$. The left side shows the undisturbed order, the right side the modified scheme for the μ^+ nearest neighbor Pr^{3+}-ions [22].

destroys the hexagonal local symmetry. This leads to the appearance of the B_2^2-term. Secondly the μ^+ Coulomb potential together with the formation of the screening cloud leads to additional electric field gradients. However, a point charge model calculation, not surprisingly, proved inappropriate to reproduce the data. As Fig. 8 shows the splitting between the ground state and the first excited level is much reduced in the presence of the μ^+. This moves the ion closer to a magnetic instability and one is tempted to predict that hydriding of $PrNi_5$ will allow for the occupance of magnetic order, possibly ferromagnetic like in other $RENi_5$ compounds. Attempts to confirm this conjecture in $PrNi_5H_\delta$ are under way but no conclusive results are yet available. Interestingly in $PrIn_3$, another singlet ground state system, K_μ seems to scale with χ_s down to 15 K and no clear indication for a μ^+ induced modification of the local susceptibility is seen [45]. However, in $PrIn_3$ the CEF splitting is much larger than in $PrNi_5$, in particular the first excited state is about a factor of five farther displaced from the ground state than in $PrNi_5$. Any μ^+ induced level shifts will therefore be much less effective in changing the local atomic susceptibility.

7. Conclusions

The presented examples demonstrate that positive muons can indeed be used to study various properties of hydrogen–metal systems. This does not only concern the behavior of hydrogen itself but also modifications induced in the metal host matrix by the presence of the muon/proton. Unique information was obtained on the quantum nature of μ^+ diffusion, revealing in particular the effect of the electron screening cloud on the elementary tunnelling event. Determination of lattice sites and associated lattice relaxations was possible in a wide variety of compounds. μ^+-Knight shift measurements in simple s-electron metals proved the ''protonic'' character of the local electronic structure. An outstanding problem in metal hydrides is the apparently smaller diffusion rate of μ^+ as compared to the diffusion rate of protons. It can be expected that μSR studies will continue to contribute to our understanding of hydrogen–metal systems.

References

[1] S.F.J. Cox and R.L. Lichti, *J. Alloys Comp., 253–254* (1997) 414–419.
[2] See e.g. P. Jena, *Treatise on Materials Science and Technology*, Vol. 21, Academic Press, New York, 1981, p. 351.
[3] E. Karlsson, *Solid State Phenomena*, Clarendon Press, Oxford, 1995.
[4] D. Richter, in *Springer Tracts in Modern Physics*, Vol 101, 1983.
[5] R. Hempelmann and D. Richter, *Europhys. News, 22* (1991) 110.
[6] A. Schenck, *Muon Spin Rotation Spectroscopy*, Adam Ailger, Bristol, 1985; J.H. Brewer, *Encyclopedia of Applied Physics*, Vol. 11, VCH Publishers, 1994.
[7] R. Feyerherm, *Thesis No. 11249*, ETH Zürich, 1995, unpublished.
[8] A. Amato, R. Feyerherm, F.N. Gygax and A. Schenck, *Hyperfine Interact*, (Proceedings of 7th International Conference on μSR, Nikko, 1996) to be published.
[9] M. Camani, F.N. Gygax, W. Rüegg, A. Schenck and H. Schilling, *Phys. Rev. Lett., 39* (1977) 836.
[10] G.M. Luke, J.H. Brewer, S.R. Kreitzman, D.R. Noakes, M. Celio, R. Kadono and A.J. Ansaldo, *Phys. Rev. B, 43* (1991) 3284.
[11] K.W. Kehr, D. Richter, J.M. Welter, O. Hartmann, E. Karlsson and L.O. Norlin, *Phys. Rev. B, 26* (1982) 567.
[12] F.N. Gygax, A. Hintermann, W. Rüegg, A. Schenck, W. Studer, A.J. van der Waal and N. Kaplan, *J. Less-Comm. Met., 101* (1984) 335.
[13] D. Herlach, V. Claus, K. Fürderer, J. Major, A. Seeger, L. Schimmele, M. Schmolz, W. Staiger, W. Templ and E. Yogi, *Z. Phys. Chem. NF, 164* (1989) 1041.
[14] A.B. Denison, H. Graf, W. Kündig and P.F. Meier, *Helv. Phys. Acta, 52* (1979) 460.
[15] F.N. Gygax, A. Amato, R. Feyerherm, A. Schenck, I.S. Anderson, T.J. Udovic and G. Solt, *J. Alloys Compds., 231* (1995) 248.
[16] F.N. Gygax, P. Birrer, B. Hitti, E. Lippelt, A. Schenck and M. Weber, *Hyperfine Interact., 64* (1990) 489.
[17] F.N. Gygax, A. Schenck, S. Barth, T. Riesterer and L. Schlapbach, *J. Less-Comm. Met., 129* (1987) 237.
[18] W.J. Kossler, H.E. Schone, K. Petzinger, B. Hitti, J. Kempton, E.F.W. Seymour, C.E. Stronach, W.F. Lankford and J.J. Reilly, *Hyperfine Interact., 31* (1986) 235.
[19] A. Schenck, A. Amato, F.N. Gygax, M. Pinkpank and H.R. Ott, *Hyperfine Interact.*, in press (see Ref. 4).
[20] O. Hartmann, R. Wäppling, A. Yaouanc, P. Dalmas de Réotier, B. Barbara, K. Aggarwal, L. Asch, A. Kratzer, G.M. Kalvius, F.N. Gygax, B. Hitti, E. Lippelt and A. Schenck, *Hyperfine Interact., 51* (1989) 955.
[21] A.M. Mulders et al., PSI-data, 1995, unpublished.
[22] R. Feyerherm, A. Amato, A. Grayevski, F.N. Gygax, N. Kaplan and A. Schenck, *Z. Phys. B, 99* (1995) 3.
[23] L.P. Le, R.H. Heffner, J.D. Thompson, D.E. MacLaughlin, G.J. Nieuwenhuys, A. Amato, R. Feyerherm, F.N. Gygax, A. Schenck, P.C. Canfield and B.K. Cho, *Phys. Rev. B, 53* (1995) 3.
[24] F.N. Gygax, B. Hitti, E. Lippelt, A. Schenck and S. Barth, *Z. Phys. B, 71* (1988) 473.1
[25] F.N. Gygax, A. Hintermann, W. Rüegg, A. Schenck, W. Studer and A.J. van der Waal, *J. Less-Comm. Met., 101* (1984) 327.
[26] P. Birrer, *Diploma Thesis*, ETH Zürich, 1987, unpublished.
[27] A. Schenck, *Helv. Phys. Acta, 54* (1981) 471; F.N. Gygax, A. Hintermann, W. Rüegg, A. Schenck, W. Studer and A.J. van der Waal, *J. Less-Comm. Met., 101* (1984) 97.
[28] M. Manninen, *Phys. Rev. B, 27* (1983) 53.
[29] F.N. Gygax, A. Hintermann, W. Rüegg, A. Schenck, W. Studer and A.J. van der Waal, *Phys. Rev. Lett., 51* (1983) 505.
[30] O. Hartmann, *Phys. Rev. Lett., 39* (1977) 832.
[31] See. e.g. S.R. Kreitzman, *Hyperfine Interact., 31* (1986) 13.
[32] M. Camani et al., SIN-Newsletter No. 7, 1976, p. 23.
[33] O. Hartmann, L.O. Norlin, A. Yaouanc, J. Le Hericy, E. Karlsson and T.O. Niinikoski, *Hyperfine Interact., 8* (1981) 533.
[34] Y. Kagan and M.I. Klinger, *J. Phys. C, 7* (1974) 2791.
[35] R. Kadono, J. Imazato, T. Matsuzaki, K. Nishiyama, K. Nagamine, T. Yamazaki, D. Richter and J.M. Welter, *Phys. Rev. B, 39* (1989) 23.
[36] J. Kondo, *Physica B, 125* (1984) 279; *126* (1984) 377.
[37] K. Yamada, *Prog. Theor. Phys., 72* (1984) 195.
[38] T. Pfiz, R. Kadono, R.F. Kiefl, S.R. Kreitzman, Q. Li and T.M. Riseman, *J. Less-Comm. Met., 172* (1991) 759.
[39] N.F. Berk, J.J. Rush, T.J. Udovic and I.S. Andersen, *J. Less-Comm. Met., 172* (1991) 496.
[40] H. Wipf, J. Steinbinder, K. Neumaier, P. Gutsmiedl, A. Magerl and A.J. Dianaux, *Europhys. Lett., 4* (1987) 1379.
[41] D. Richter, R. Hempelmann, O. Hartmann, E. Karlsson, L.O. Norlin, S.F.J. Cox and R. Kutner, *J. Chem. Phys., 79* (1983) 4564.

[42] A. Baudry, P. Boyet, A. Chikdene, S.W. Harris and S.F.J. Cox, *Hyperfine Interact., 64* (1990) 657.
[43] R. Hempelmann, D. Richter, O. Hartmann and R. Wälppling, *Hyperfine Interact., 64* (1990) 649.
[44] P. Birrer, F.N. Gygax, B. Hitti, E. Lippelt and A. Schenck, *Z. Phys. Chem. NF, 164* (1989) 1047.
[45] A. Grayevski, I. Felner, T. Tashama, N. Kaplan, F.N. Gygax, A. Amato, M. Pinkpank and A. Schenck, *Hyperfine Interact*., in press (see Ref. 4).